ELSEVIER

Biophysical Chemistry 122 (2006) 36–42

Biophysical Chemistry

http://www.elsevier.com/locate/biophyschem

Effect of externally applied electrostatic fields on the surface topography of ceramide-enriched domains in mixed monolayers with sphingomyelin

Natalia Wilke, Bruno Maggio *

Departamento de Química Biológica-CIQUIBIC, Facultad de Ciencias Químicas, Universidad Nacional de Córdoba, Ciudad Universitaria, 5000 Córdoba, Argentina

Received 14 October 2005; received in revised form 14 February 2006; accepted 16 February 2006
Available online 9 March 2006

Abstract

Lipid and protein molecules anisotropically oriented at a hydrocarbon–aqueous interface configure a dynamic array of self-organized molecular dipoles. Electrostatic fields applied to lipid monolayers have been shown to induce in-plane migration of domains or phase separation in a homogeneous system. In this work, we have investigated the effect of externally applied electrostatic fields on the distribution of the condensed ceramide-enriched domains in mixed monolayers with sphingomyelin. In these monolayers, the lipids segregate in different phases at all pressures. This allows analyzing by epifluorescence microscopy the effect of the electrostatic field at all lateral pressure because coexistence of lipid domains in condensed state are always present. Our observations indicate that a positive potential applied to an electrode placed over the monolayer promotes a repulsion of the ceramide-enriched domains which is rather insensitive to the film composition, depends inversely on the lateral pressure and exhibits threshold dependence on the in-plane elasticity.

Keywords: Electric field; Lipid monolayer; Sphingomyelin; Ceramide

1. Introduction

Lipid and protein molecules anisotropically oriented at a hydrocarbon–aqueous interface such as that existing in biomembranes configure a dynamic array of self-organized molecular dipoles. These can act as sensitive local and long-range sensors of the electrical properties along and across the membrane interface [1]. Intrinsic electrostatic features, intermolecular packing and interactions determine a resultant dipole moment density that in conjunction with line tension forces are major factors responsible for the individual morphology of coexisting phase domains as well as their lattice organization along the surface [2].

Constant or alternating electromagnetic fields of different intensities can induce dramatic effects in biosystems [3]. This is not surprising in view of the marked molecular and supramolecular anisotropy that is inherent to polarized molecules in biomembranes. Varied effects include dynamic modifications of membrane topology [4–6], cellular function [7,8], protein phosphorylation [9] as well as activation of membrane-associated enzymes [10–15]. The formation and response of selective domain morphology with boundary defects and lattice super-structuring through the control of dipole-generated electrostatic fields along the lateral and across the transverse planes of the membrane surface appear as important regulatory mechanisms for lipase catalysis [11,12,16–18], phospholipase interfacial location [19], phase transitions and lateral domain migration [20–23], and channel conductance [24–26]. Regarding shingolipids, changes of hydration, charge and/or molecular tilting in galactocerebroside- and sulfatide-containing films can be amplified to alterations of the phase state and domain topography [27–29]. We have previously shown that reversible surface reorganization of galactocerebroside occurred with marked hysteresis depending on the sign and magnitude of the electrostatic potential applied [30]. In a recent work, it was also demonstrated the importance of the dipole moment density difference among the immiscible sphingomyelin and ceramide monolayer, coupled to the domain boundary line tension, to establish both the characteristic domain morphology and their

* Corresponding author. Tel.: +54 351 4334168; fax: +54 351 4334074.
E-mail address: bmaggio@mail.fcq.unc.edu.ar (B. Maggio).

0301-4622/$ - see front matter © 2006 Elsevier B.V. All rights reserved.
doi:10.1016/j.bpc.2006.02.008

lattice organization in premixed binary films and in those generated by the action of sphingomyelinase [2]. In the present work, we have investigated the effect of externally applied electrostatic fields on the distribution of the condensed ceramide-enriched domains in mixed monolayers with different sphingomyelin proportions.

2. Experimental section

2.1. Materials

Bovine brain sphingomyelin (Sm), ceramide (Cer) and the lipophilic fluorescent probe L-α-phosphatidylethanolamine-*N*-(lissamine rhodamine B sulfonyl)–Ammonium Salt (RhoPE) were purchased from Avanti Polar Lipids (Alabaster, AL, USA). Solvents and chemicals were of the highest commercial purity available. The water used for the subphase was double distilled in an all-glass apparatus. Lipid monolayers were prepared and characterized in an automated equipment as described elsewhere [31]. Several measurements were performed for the compression isotherms; the results shown represent average values and reproducibility was within 5%.

2.2. Methods

2.2.1. Brewster angle measurements

Brewster Angle Microscopy (BAM) observations and image analysis were carried out as described before [32]. At the Brewster angle, the relative thickness at a defined surface pressure can be derived from relative reflectance measurements:

$$\frac{d}{d_{\pi=0}} = \sqrt{\frac{I}{I_{\pi=0}}} \quad (1)$$

where I and d are the reflectance and the film thickness at a given lateral pressure, respectively. $I_{\pi=0}$ and $d_{\pi=0}$ are the intensity and the thickness at 0 mN m^{-1}.

2.2.2. Epifluorescence microscopy of monolayers

RhoPE was incorporated into the lipid solution before spreading (0.5 mol%). The monolayer was compressed up to 35 mN m^{-1} (a high pressure at which the layer is in an all-condensed state, with high cohesion, but still well before collapse), decompressed to 0 mN m^{-1} and then taken to the desired lateral pressure. A micrograph was taken at the chosen pressure before applying the electrostatic field. The observations were carried out at room temperature (24 ± 1 °C), using a glass through (microthrough, Kibron, Helsinki, Finland). An open-end Teflon mask with lateral slits covering the objective and extending through the film into the subphase was used to restrict lateral monolayer flow under the field being observed. A Zeiss Axiovert-200 (Carl Zeiss, Oberkochen, Germany) epifluorescence microscope with a source of radiation provided by a mercury lamp HBO 50 and a rhodamine filter set were used. Images were registered by a CCD video camera AxioCam HRc (Zeiss) commanded through the Axiovision 3.1 software of the Zeiss microscope. Objectives of 20×, 5.6× and 3.2× were used.

2.2.3. Electrostatic field setup

The experimental setup for applying the electrostatic field was similar to that used in Heckl et al. [22]. It consists in a Pt wire inserted in the subphase and a metal wire of 30 μm in diameter held at 150–200 μm of the subphase (see Scheme 1); while the monolayer topography is continuously observed from above, the upper electrode can be manipulated over the monolayer by moving it into three orthogonal directions with a micromanipulator (Carl Zeiss, Oberkochen, Germany) to an accuracy of 10 μm. The electrode can be charged to apply potentials of up to ±300 V with respect to the subphase electrode. This was performed with a BioRad pac 300 constant power supply.

2.2.4. Computational analysis of surface topography

The lipophilic fluorescent probe RhoPE shows preferential partition in the Sm-enriched zones of the lipid monolayer [33]. In Sm : Cer mixed monolayers, the Cer-enriched domains are in a more condensed and ordered state than the Sm-enriched zones, thus excluding the fluorescent probe. In the images recorded before applying the electrostatic field, segmentation of RhoPE-depleted areas was achieved by interactive image

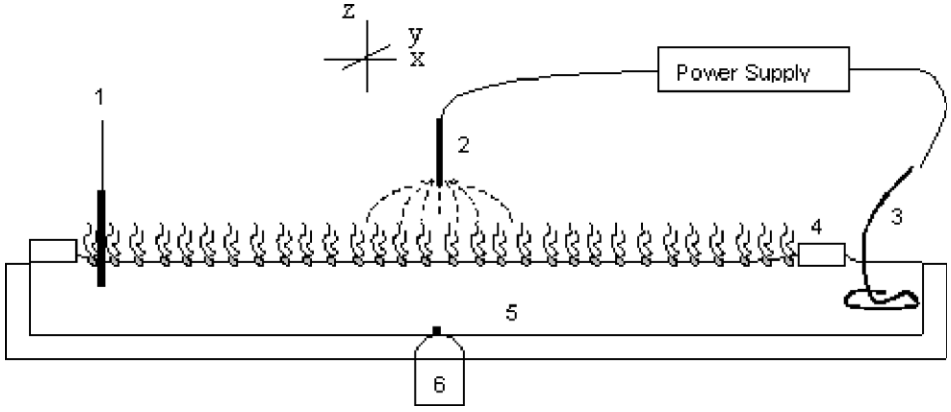

Scheme 1. Experimental set up (not in scale). A Langmuir monolayer is spread on an aqueous surface in a glass trough that is mounted on an inverted microscopy. 1 – Wilhelmy plate, 2 – upper electrode and qualitative electric field lines. The electrode can be displaced in the three orthogonal directions with a micromanipulator: 3 – Pt electrode, 4 – PTFE barriers, 5 – subphase : electrolytic solution, 6 – microscope objective.

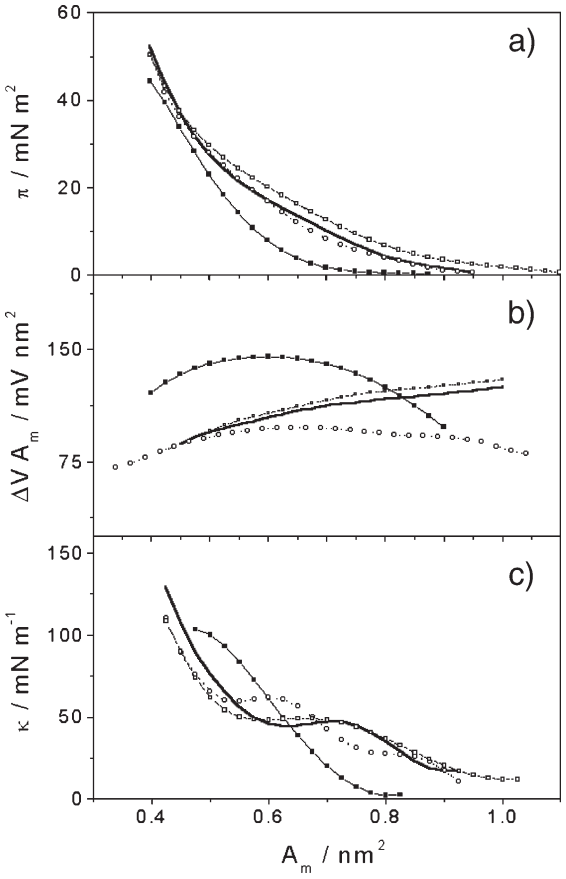

Fig. 1. Compression isotherm for monolayers composed of pure Cer, pure Sm or Sm : Cer mixtures. (a) Lateral pressure as a function of the molecular area. (b) Surface potential density as a function of the molecular area. (c) In-plane elasticity as a function of the molecular area. Pure Cer (–■–), pure Sm (—), Sm : Cer mixtures: 80 : 20 (··○··), 90 : 10 (–□–).

processing routines written in IDL (Interactive Data Language, Research Systems Co.; Boulder, CO, USA). The protocol for image analysis was described elsewhere [2].

3. Results

Fig. 1 shows the compression isotherms for each mixture and for the pure lipids over 0.145 M NaCl. Fig. 1a shows the lateral pressure π vs. the mean molecular area A_m, Fig. 1b shows the dipole potential density ΔVA_m vs. the mean molecular area A_m and Fig. 1c shows the in-plane elasticity κ (calculated as described in Wilke et al. [34]) vs. the mean molecular area A_m. As previously described [33], Sm shows a two dimensional phase transition, from an expanded to a condensed phase, in the range of 10–27 mN m^{-1} and collapses at 58 mN m^{-1} with a limiting mean molecular area of 0.47 nm^2. The dipole potential density is in the range of 150–170 mV nm^2 and it shows only slight changes along the compression isotherm. κ shows a minimum at around 0.62 nm^2 corresponding to the phase change. Cer is in a condensed state [32]. The isotherm shows a collapse at 40 mN m^{-1} with a molecular area of 0.41 nm^2. The dipole potential density is somewhat higher than for Sm and changes during the compression isotherm. κ increases monotonically up to the monolayer collapse.

The Cer–Sm mixtures follow an ideal behavior; this is expected either for ideally mixed or fully immiscible components [35]. In the present case, the two-dimensional phase diagram indicates that both lipids are hardly miscible (less than 10%) [33]. For the mixed film containing 20 mol% Cer – 80 mol% Sm, the phase transition at 10–27 mN m^{-1} cannot be detected from the π–A_m compression isotherm but becomes evident in the κ–A_m plot, occurring at higher κ values than for the pure Sm monolayer. For both proportions of Sm : Cer, the lipids segregate in different phases at all pressures, as evidenced by epifluorescence microscopy, where two phases are observed at every pressure (Fig. 2a–d). This feature of the mixture allows analyzing the effect of the electrostatic field at all lateral pressure because Cer-enriched domains are always present.

When an electrostatic field is applied to the Cer–Sm monolayers exhibiting phase coexistence the following general effects are observed. If a positive potential is applied to the upper electrode, a repulsion of the dark domains from the area of influence of the electrode over the monolayer is induced (Fig. 2e); by contrast, the application of a negative potential causes domain attraction (Fig. 2f). These results coincide qualitatively with that observed by Heckl et al. [22] and by Klinger and McConnell using other lipid systems [21]. Despite the potentials we are applying are higher compared to those in Heckl et al. [22], as the upper electrode is at a higher distance from the interface, the resulting potential gradients are similar. In this paper, we explored the effect of positive potential applied to the upper electrode at different lateral pressures and for different lipid monolayer compositions.

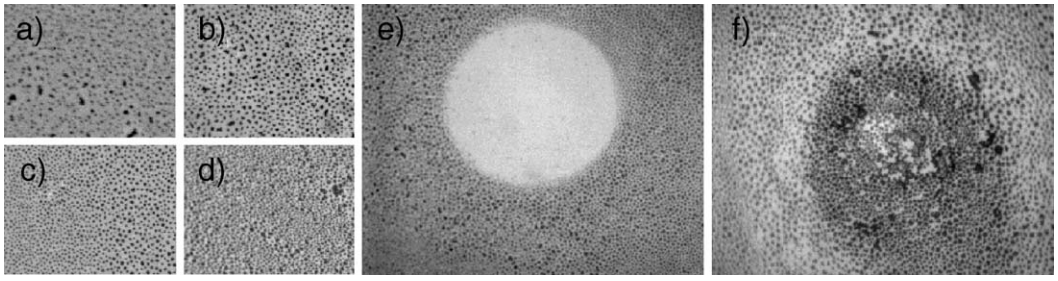

Fig. 2. Epifluorescence microscopy for a Sm : Cer (90 : 10) monolayer over 0.145 M NaCl at room temperature. The lateral pressures are: (a) 0 mN m^{-1}, (b) 10 mN m^{-1}, (c) 20 mN m^{-1}; (d) 35 mN m^{-1}. Real size: 325 × 260 μm^2. In micrographs (e) and (f), an electric field has been applied at 20 mN m^{-1}. The upper electrode is held at +300 V in (e) and −300 V in (f) with respect to the subphase electrode. Real size: 650 × 520 μm^2.

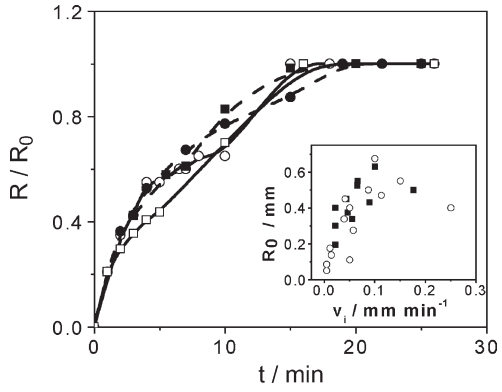

Fig. 3. Radius (R) of the area devoid of domains normalized by the final radius (R_0) as a function of time for different conditions. Sm:Cer=90:10 at 10 mN m^{-1} (○) and at 20 mN m^{-1} (●), Sm:Cer=80:20 at 0 mN m^{-1} (□) and at 20 mN m^{-1} (■). Inset: R_0 as a function of the initial velocity of formation of the area devoid of domains, Sm:Cer=80:20 (■) and 90:10 (○).

When a positive potential is applied to the upper electrode, the dark domains begin to move away from the electrode-affected region, forming a round zone devoid of condensed domains of radius R. This process is reverted when the potential is switched off. R increases with time until a maximum radius R_0 is reached. This process is shown in Fig. 3, where $R(t)/R_0$ is plotted as a function of time for four independent experiments at different lateral pressures and for different lipid monolayer compositions. As can be deduced from Fig. 3, the time at which the final R is achieved is independent on the lateral pressure and on the lipid monolayer composition. This implies that the larger R_0, the higher the velocity at which R increases (see inset of Fig. 3).

Fig. 4a shows the R_0 values as a function of the lateral pressure for the two lipid monolayers compositions studied (90 mol%, 80 mol% Sm and 10 mol%, 20 mol% Cer, respectively). Each value in this figure corresponds to an independent experiment; duplicate values for R_0 are shown for most pressures. A monotonical decrease of R_0 is found up to 20 mN m^{-1} for both lipid compositions. At higher surface pressures the one containing 20 mol% Cer continues with the same monotonical behavior, while the other decays abruptly. This latter can be related with the phase transition exhibited in the compression isotherm (Fig. 1a), and which is not so evident in the film with 20 mol% Cer.

4. Discussion

The movement of a given domain depends on the force applied on it and on the forces opposing its movement. The force on the domain is that of a dipole in an inhomogeneous field and is given by Eq. (2) [36]

$$F_x = -\overrightarrow{P}\cdot\nabla E_x \tag{2}$$

Eq. (2) applies to each space coordinate of the system. In other words, the force on some coordinate x depends on the gradient of the component of field over that coordinate ∇E_x, on the lipid dipole moment $\overrightarrow{p}(\overrightarrow{P}=n\overrightarrow{p})$ and on the amount of dipoles forming the domain (n). The forces opposing the domain movement are related with the viscosity of the film, the repulsion between the condensed domains and the thermal energy. Therefore, the lateral pressure dependence of R_0 involves changes of dipole moment under compression, domain size (n), viscosity and/or amount of nearest neighbor domains (thus on the lattice type). The applied electrostatic field was similar in each experiment.

To analyze the size and amount of domains, all the micrographs taken before applying the electrostatic field were quantified. Their topography was analyzed as explained in Methods. We found that neither the sizes nor the amount of the dark domains change with the lateral pressure, indicating that n is not changing with π. The dark area percentage is larger than that expected for total lipid immiscibility. This was observed before [33] and this indicates that the dark domains are Cer-enriched but not pure Cer domains. The number of nearest neighbors (type of lattice) and the distance between the closest domains are the same at any condition and show a high dispersion of values, typical of a random array, indicating that the repulsion between domains is not the factor that is changing with π and that is responsible for the variation of R_0.

The repulsive force depends also on the molecular dipole moment p of the lipid molecules forming the domain. A decrease of the p components decreases the repulsive force. The

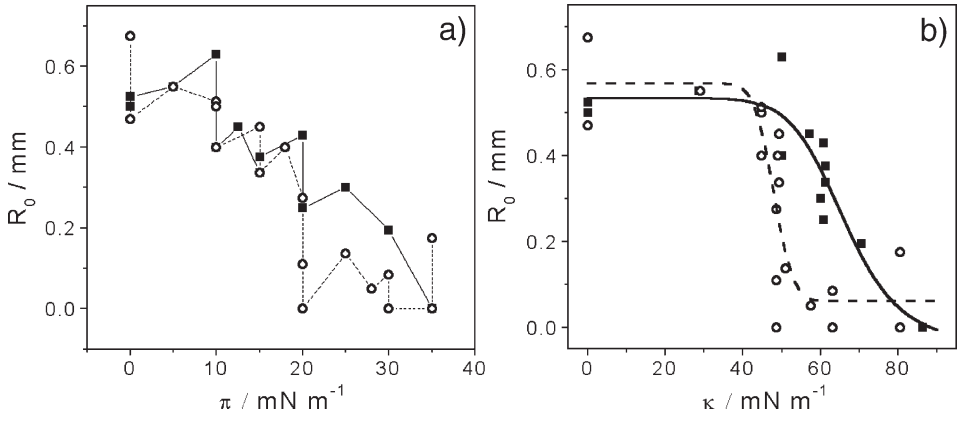

Fig. 4. Final radius (R_0) of the area devoid of domains as a function of (a) the lateral pressure and (b) the in-plane elasticity. Sm:Cer=80:20 (■) and 90:10 (○).

techniques available for measuring dipole potential in Langmuir monolayer systems only allow to calculate the dipole moment normal to the interface p^N. A change in p^N would promote a change of the dipole potential density (ΔVA_m). Fig. 1 shows that for Cer, ΔVA_m increases up to a maximum value at a mean molecular area of 0.54 nm^2 and then decreases. If it is considered that the dark domain behaves as pure Cer, a similar tendency would be expected in R_0 (unless different effects are compensating each other) but this is not the case. Thus we conclude that this is not the principal factor that promotes the R_0 dependence on π shown in Fig. 4a. A dipole moment component parallel to the interface could pre-exist or be induced by the electrostatic field; unfortunately, this is not possible to ascertain or measure explicitly with our current experimental set up.

At this stage, we have shown that the parameters that describe the domain properties remain unchanged or show only slight changes with the lateral pressure. Regarding the parameters related to the continuous phase properties, Fig. 4b shows the general variation of R_0 with the surface in-plane elasticity κ depicted previously in Fig. 1c. There is a rather narrow κ-values range (between 50 and 70 mN/m) from which the size of the domain-free region induced by a same electrostatic field intensity is either facilitated (at low κ values, corresponding to a more fluid compressible films) or impaired (at high κ values, corresponding to a more condensed incompressible monolayer). Between 50 and 70 mN/m, R_0 shows large changes with small κ changes. This range of κ values corresponds to those in which the monolayer phase transition takes place, where the monolayer rheology undergoes conspicuous change, and R_0 also varies in a sharp way. The plot shows that the change of R_0 with κ is more abrupt for the film with 10 mol% Cer than for that with 20 mol% Cer and occurs at lower κ values. This is consistent with the lower values of κ in the phase transition and with the more cooperative phase change for the mixture with 10 mol% Cer.

The R_0 dependence on the in-plane elasticity indicates that the monolayer rheology affects the electrostatic field effect.

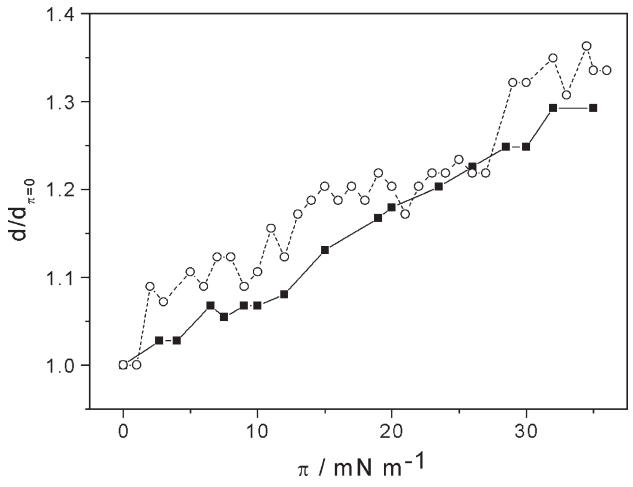

Fig. 5. Relative film thickness as a function of the lateral pressure. Sm:Cer=80:20 (■) and 90:10 (○).

Changes of viscosity of the monolayer, dependent on the surface pressure, could indeed affect the velocity at which the domain-free area is formed, and therefore, the R_0 value. Besides, the relative thickness of the monolayer increases as the lateral pressure increases as revealed by BAM (Fig. 5). This also implies that as the surface pressure increases, the proportion of lateral surface of the dark domains in contact with the rest of the monolayer is larger and the surface viscosity may become important for influencing domain displacement.

5. Conclusions

In monolayers of Sm:Cer, the lipids segregate in different phases at all pressures. This feature makes this mixture a good system for analyzing field effects as dark domains are always present. Cer-enriched domains in a Sm-enriched media behave like other mixtures in the sense that positive potentials applied to the upper electrode reversibly repel the domains and negative potentials attract them.

The observed field effects strongly depend on the lateral pressure. None of the analyzed parameters that describe the domain properties show significant changes with the lateral pressure. A dipole moment component parallel to the interface dependent on pressure is suggested by the induced electrostatic response of the lateral domain topography but, unfortunately, this is not possible to ascertain or measure explicitly with our current experimental set up.

As none of the measured parameters describing the domain properties change with the lateral pressure, it is possible that some property related to the continuous phase impairs domain movement at high lateral pressures. The dependence of R_0 with the in-plane elasticity shows a sharp change over the values of κ in the phase transition range. This indicates that the monolayer viscosity could be a major factor that modifies the field effect in a surface pressure-dependent manner and this is currently under investigation. Heckl et al. have shown [22] that for domains of around 30 μm^2 size, the subphase viscosity is more important than the monolayer viscosity to describe the domain movement 3 in an electrostatic field. In our case, the domain size is 12±6 μm^2, which implies that the area in contact with the monolayer is only 2% of the total domain area (assuming a monolayer thickness of 20 nm). However, by only considering thickness changes, the area percentage of the domain in contact with the monolayer would increase about 1.4 times from π=0 mN m^{-1} to π=35 mN m^{-1}. Since the viscosity of the monolayer also changes during the compression (an increase is expected, as indicated by the increase of the in-plane elasticity), the monolayer rheology appears as a factor more important than composition or domain morphology to modulate the field-induced effects.

Cellular processes such as receptor-mediated ligand response, cell proliferation, differentiation, and death are triggered by the locally and temporally stimulated enzymatic conversion of Sm to Cer [24,37,38]. Besides the conception of Cer as an important second messenger [39,40], there are direct short- and long-range structural consequences of the Sm–Cer

conversion in biomembranes through the formation of segregated Cer-enriched domains [2,33,41,42] and the distribution/clearance of Sm-enriched membrane rafts [43]. Secondary structural consequences of lateral organization of Cer-enriched domains are related to permeability [44], bilayer lipid translocation [45], formation of apoptotic bodies [46] and cellular signaling through channel activation [24] or phospholipid breakdown [47,48].

Among other effects, lateral distribution of lipid domains with boundary defects and specific dipole moments can control membrane lipid composition and sphingolipid asymmetry [45] through the modulation and cross-regulation of membrane-active lipolytic enzymes [2,12,33,49–52]. Cer-enriched domains actively formed by sphingomyelinase segregate and organize at random or in lateral super-lattices in a matrix of Sm depending on their surface density and morphologic features. These structural parameters are coupled to the generation of repulsive lateral two-dimensional electrostatic fields at the domain boundaries ranging between about 30 and 3000 V/m that arise from the specific orientation of the lipid dipole moments. In our experiments, the force generated on the domains by an electrode held at 300 V, with respect to the subphase, is maximal at 100 μm from the electrode. A protein such as melittin, at a molecular area of 1.78 nm^2 generates a surfase potential of 465 mV [53]; thus, this protein would generate forces similar to the electrode at 0.1 μm from the protein (about 280 lipid molecular diameter in lateral distance). In other words, in nature the cell membrane bears field gradients of the order of magnitude as that applied with our experimental setup.

The distance between the Cer-enriched domains is a major factor to determine the inter-domain repulsive electrostatic energy in relation to the thermal energy; this ratio is a critical factor to establish an ordered organization of domain super-lattices with a high content and capacity to transduce structural and biocatalytic information from the nm to the μm scale ranges via the repulsive lateral electrostatic field resulting from the intrinsic dipole moment density differences (in the order of 0.1–1.0 Debye/nm^2) among the domain and the rest of the lipid matrix [2]. It was previously shown that the lateral organization of Cer-enriched domains in the Sm matrix is a consequence of, and subsequently controls, the variation of such field thus becoming a self-amplifying bio-catalytic-electrochemical factor driving the structural dynamics of the membrane surface; the rather strong electrostatic field gradient a the domain boundaries, depending on their morphology, can constitute potential attractive or repulsive traps for laterally diffusing molecules as well as a major factor for inter-domain structuring in defined super-lattices [2].

Our results now demonstrate directly the dipolar nature of Cer-enriched segregated domains, the sensitivity of their surface dynamics to externally imposed electrostatic field gradients, and that their response can be modulated by the surface free energy (lateral surface pressure) and interfacial elasticity. This allows to begin dissecting the synergetics of the cascade of biophysical events underlying the membrane structural dynamics, thus making possible to attempt narrowing the gap between local molecular events (on the nm scale range) and the supramolecular (μm scale range) of membrane-mediated cellular function.

Acknowledgments

This work was supported by SECyT-UNC, Fundacion Antorchas, CONICET and FONCYT, Argentina. N. W. is a postdoctoral fellow of CONICET, and B.M. is Superior Career Investigator of CONICET.

References

[1] J. Seelig, P.M. Mcdonald, P.G. Scherer, Phospholipid head groups as sensors of electric charge in membranes, Biochemistry 26 (1987) 7535–7541.
[2] S. Hartel, M.L. Fanani, B. Maggio, Shape transitions and lattice structuring of ceramide-enriched domains generated by sphingomyelinase in lipid monolayers, Biophys. J. 88 (2005) 287–304.
[3] M.J. Allen, S.F. Cleary, A.E. Sowers, D.D. Shillady, Charge and Field Effects in Biosystems-3, Birkhauser, Boston, 1992.
[4] G. Stulen, Electric field effects on lipid membrane structure, Biochim. Biophys. Acta 640 (1981) 621–627.
[5] J. Teissie, T.Y. Tsong, Electric field induced transient pores in phospholipid bilayer vesicles, Biochemistry 20 (1981) 1548–1554.
[6] A. Lopez, M.P. Rols, J. Teissie, ^{31}P NMR analysis of membrane phospholipid organization in viable, reversibly electropermeabilized Chinese hamster ovary cells, Biochemistry 27 (1988) 1222–1228.
[7] M.S. Markov, J.T. Ryoby, J.J. Kauffman, A.A. Pilla, in: M.J. Allen, S. F. Cleary, A.E. Sowers, D.D. Shillady (Eds.), Extremely Weak AC and DC Magnetic Fields Significantly Affect Myosin Phosphorylation, Charge and Field Effects in Biosystems-3, Birkhauser, Boston, 1992, pp. 225–230.
[8] S.F. Cleary, L.-M. Liu, G. Cao, in: M.J. Allen, S.F. Cleary, A.E. Sowers, D. D. Shillady (Eds.), Cellular Effects of Extremely Low Frequency Electromagnetic Fields, Charge and Field Effects in Biosystems-3, Birkhauser, Boston, 1992, pp. 203–217.
[9] S. Kwee, P. Roskmark, in: M.J. Allen, S.F. Cleary, A.E. Sowers (Eds.), Changes in Cell Proliferation Due to Environment Electromagnetic Fields, Charge and Field Effects in Biosystems-4, World Scientific Pub. Co., Singapur, 1994, pp. 255–259.
[10] T.Y. Tsong, Electrical modulation of membrane proteins: enforced conformational oscillations and biological energy and signal transductions, Annu. Rev. Biophys. Biophys. Chem. 19 (1990) 83–106.
[11] T. Thuren, A.P. Tulkki, J.A. Virtanen, P.K. Kinnunen, Triggering of the activity of phospholipase A_2 by an electric field, Biochemistry 26 (1987) 4907–4910.
[12] B. Maggio, Modulation of phospholipase A_2 by electrostatic fields and dipole potential of glycosphingolipids in monolayers, J. Lipid Res. 40 (1999) 930–939.
[13] T.Y. Tsong, R.D. Astumian, Electroconformational coupling: how membrane-bound ATPase transduces energy from dynamic electric fields, Annu. Rev. Physiol. 50 (1988) 273–290.
[14] D.S. Liu, R.D. Astumian, T.Y. Tsong, Activation of Na^+ and K^+ pumping modes of (Na,K)-ATPase by an oscillating electric field, J. Biol. Chem. 265 (1990) 7260–7267.
[15] A. Graziana, R. Ranjeva, J. Teissie, External electric fields stimulate the electrogenic calcium/sodium exchange in plant protoplasts, Biochemistry 29 (1990) 8313–8318.
[16] D.W. Grainger, A. Reichert, H. Ringsdorf, C. Salesse, Hydrolytic action of phospholipase A_2 in monolayers in the phase transition region: direct observation of enzyme domain formation using fluorescence microscopy, Biochim. Biophys. Acta 1023 (1990) 365–379.
[17] J.M. Muderhwa, H.L. Brockman, Lateral lipid distribution is a major regulator of lipase activity. Implications for lipid-mediated signal transduction, J. Biol. Chem. 267 (1992) 24184–24192.

[18] M.M. Wang, M. Olsher, I.P. Sugar, P.L. Chong, Cholesterol superlattice modulates the activity of cholesterol oxidase in lipid membranes, Biochemistry 43 (2004) 2159–2166.
[19] Y. Lin, R. Nielsen, D. Murray, W.L. Hubbell, C. Mailer, B.H. Robinson, M.H. Gelb, Docking phospholipase A_2 on membranes using electrostatic potential-modulated spin relaxation magnetic resonance, Science 279 (1998) 1925–1929.
[20] K.Y. Lee, H.M. McConnell, Effect of electric field gradients on lipid monolayer membranes, Biophys. J. 68 (1995) 1740–1751.
[21] J.F. Klinger, H.M. McConnell, Field-gradient electrophoresis of lipid domains, J. Phys. Chem. 97 (1993) 2962–2966.
[22] W. M. Heckl, A. Miller, H. Möhwald, Electric-field-induced domain movement in phospholipid monolayers. Thin Solid Films 159, 125–132. 88.
[23] P. Nassoy, W.R. Birch, D. Andelman, F. Rondelez, Hydrodynamic mapping of two-dimensional electric fields in monolayers, Phys. Rev. Lett. 76 (1996) 455–458.
[24] I. Szabo, C. Adams, E. Gulbins, Ion channels and membrane rafts in apoptosis, Pflugers Arch. 448 (2004) 304–312.
[25] E. Moczydlowski, O. Alvarez, C. Vergara, R. Latorre, Effect of phospholipid surface charge on the conductance and gating of a Ca^{2+}-activated K^+ channel in planar lipid bilayers, J. Membr. Biol. 83 (1985) 273–282.
[26] J.B. Park, H.J. Kim, P.D. Ryu, E. Moczydlowski, Effect of phosphatidylserine on unitary conductance and Ba^{2+} block of the BK Ca^{2+}-activated K^+ channel: re-examination of the surface charge hypothesis, J. Gen. Physiol. 121 (2003) 375–397.
[27] B. Maggio, The surface behavior of glycosphingolipids in biomembranes: a new frontier of molecular ecology, Prog. Biophys. Mol. Biol. 62 (1994) 55–117.
[28] A. Nabet, J.M. Boggs, M. Pezolet, Study by infrared spectroscopy of the interdigitation of C26:0 cerebroside sulfate into phosphatidylcholine bilayers, Biochemistry 35 (1996) 6674–6683.
[29] K. Saxena, R.I. Duclos, P. Zimmermann, R.R. Schmidt, G.G. Shipley, Structure and properties of totally synthetic galacto- and gluco-cerebrosides, J. Lipid Res. 40 (1999) 839–849.
[30] N. Wilke, A.M. Baruzzi, B. Maggio, M.A. Perez, M.L. Teijelo, Properties of galactocerebroside layers transferred to glassy carbon electrodes: effect of an applied electric field, Colloids Surf., B Biointerfaces 41 (2005) 223–231.
[31] M.F. Mora, N. Wilke, A.M. Baruzzi, Electron-transfer processes at electrodes covered by lipid layers. Correlation with the lipid behavior at the air–water interface, Langmuir 19 (2003) 6876–6880.
[32] C.M. Rosetti, R.G. Oliveira, B. Maggio, Reflectance and topography of glycosphingolipid monolayers at the air–water interface, Langmuir 19 (2003) 377–384.
[33] M.L. Fanani, S. Hartel, R.G. Oliveira, B. Maggio, Bidirectional control of sphingomyelinase activity and surface topography in lipid monolayers, Biophys. J. 83 (2002) 3416–3424.
[34] N. Wilke, A.M. Baruzzi, B. Maggio, Sphingolipid monolayers on the air–water interface and electrochemical behavior of the films transferred onto glassy carbon electrodes, Langmuir 17 (2001) 3980–3986.
[35] G.L. Gaines, Insoluble Monolayers at Liquid–Gas Interfaces, Terscience Publishers, New York, 1966.
[36] E.M. Purcell, Electricidad y Magnetismo. Berkeley Physics Course: Volume 2, Reverte S.A., Berkeley, 1992.
[37] T. Levade, J.P. Jaffrezou, Signalling sphingomyelinases: which, where, how and why? Biochim. Biophys. Acta 1438 (1999) 1–17.
[38] Y.A. Hannun, C. Luberto, Ceramide in the eukaryotic stress response, Trends Cell Biol. 10 (2000) 73–80.
[39] R.N. Kolesnick, F.M. Goni, A. Alonso, Compartmentalization of ceramide signaling: physical foundations and biological effects, J. Cell. Physiol. 184 (2000) 285–300.
[40] F.M. Goni, F.X. Contreras, L.R. Montes, J. Sot, A. Alonso, Biophysics (and sociology) of ceramides, Biochem. Soc. Symp. (2005) 177–188.
[41] J.M. Holopainen, M.I. Angelova, P.K. Kinnunen, Vectorial budding of vesicles by asymmetrical enzymatic formation of ceramide in giant liposomes, Biophys. J. 78 (2000) 830–838.
[42] J.M. Holopainen, M. Subramanian, P.K. Kinnunen, Sphingomyelinase induces lipid microdomain formation in a fluid phosphatidylcholine/sphingomyelin membrane, Biochemistry 37 (1998) 17562–17570.
[43] E. Gulbins, S. Dreschers, B. Wilker, H. Grassme, Ceramide, membrane rafts and infections, J. Mol. Med. 82 (2004) 357–363.
[44] M.B. Ruiz-Arguello, G. Basanez, F.M. Goni, A. Alonso, Different effects of enzyme-generated ceramides and diacylglycerols in phospholipid membrane fusion and leakage, J. Biol. Chem. 271 (1996) 26616–26621.
[45] F.X. Contreras, A.V. Villar, A. Alonso, R.N. Kolesnick, F.M. Goni, Sphingomyelinase activity causes transbilayer lipid translocation in model and cell membranes, J. Biol. Chem. 278 (2003) 37169–37174.
[46] A.D. Tepper, P. Ruurs, T. Wiedmer, P.J. Sims, J. Borst, W.J. van Blitterswijk, Sphingomyelin hydrolysis to ceramide during the execution phase of apoptosis results from phospholipid scrambling and alters cell-surface morphology, J. Cell Biol. 150 (2000) 155–164.
[47] R.H. Michell, Inositol phospholipids and cell surface receptor function, Biochim. Biophys. Acta 415 (1975) 47–81.
[48] M.J. Wakelam, T.R. Pettitt, P. Kaur, C.P. Briscoe, A. Stewart, A. Paul, A. Paterson, M.J. Cross, S.D. Gardner, S. Currie, et al., Phosphatidylcholine hydrolysis: a multiple messenger generating system, Adv. Second Messenger Phosphoprot. Res. 28 (1993) 73–80.
[49] P. Somerharju, J.A. Virtanen, K.H. Cheng, Lateral organisation of membrane lipids. The superlattice view, Biochim. Biophys. Acta 1440 (1999) 32–48.
[50] P.L. Chong, I.P. Sugar, Fluorescence studies of lipid regular distribution in membranes, Chem. Phys. Lipids 116 (2002) 153–175.
[51] F. Liu, P.L. Chong, Evidence for a regulatory role of cholesterol superlattices in the hydrolytic activity of secretory phospholipase A_2 in lipid membranes, Biochemistry 38 (1999) 3867–3873.
[52] M.L. Fanani, B. Maggio, Mutual modulation of sphingomyelinase and phospholipase A_2 activities against mixed lipid monolayers by their lipid intermediates and glycosphingolipids, Mol. Membr. Biol. 14 (1997) 25–29.
[53] G.D. Fidelio, B. Maggio, F.A. Cumar, Interaction of soluble and membrane proteins with monolayers of glycosphingolipids, Biochem. J. 203 (1982) 717–725.